

Infrared identification of 2XMM J191043.4+091629.4

J. J. Rodes-Roca^{1,2}, J. M. Torrejón^{1,2}, S. Martínez-Núñez², G. Bernabéu^{1,2}, and A. Magazzú³

¹ Department of Physics, Systems Engineering and Signal Theory, University of Alicante, 03080 Alicante, Spain
e-mail: rodes@dfists.ua.es

² University Institute of Physics Applied to Sciences and Technologies, University of Alicante, 03080 Alicante, Spain

³ Telescopio Nazionale Galileo, Rambla José Ana Fernández Pérez, 38712 Breña Baja, Spain

Received ; accepted

ABSTRACT

Context. We report the infrared identification of the X-ray source 2XMM J191043.4+091629.4, which was detected by *XMM-Newton*/*EPIC* in the vicinity of the Galactic supernova remnant W49B.

Aims. The aim of this work is to establish the nature of the X-ray source 2XMM J191043.4+091629.4 studying both the infrared photometry and spectroscopy of the companion.

Methods. We analysed UKIDSS images around the best position of the X-ray source and obtained spectra of the best candidate using *NICS* in the *Telescopio Nazionale Galileo* (TNG) 3.5-m telescope. We present photometric and spectroscopic TNG analyses of the infrared counterpart of the X-ray source, identifying emission lines in the *K*-band. The *H*-band spectra does not present any significant feature.

Results. We have shown that the Brackett γ H I at 2.165 μm , and He I at 2.184 μm and at 2.058 μm are significantly present in the infrared spectrum. The CO bands are also absent from our spectrum. Based on these results and the X-ray characteristics of the source, we conclude that the infrared counterpart is an early B-type supergiant star with an $E(B - V) = 7.6 \pm 0.3$ at a distance of 16.0 ± 0.5 kpc. This would be, therefore, the first high-mass X-ray binary in the Outer Arm at galactic longitudes of between 30° and 60° .

Key words. X-rays: binaries – stars: pulsars: individual: 2XMM J191043.4+091629.4

1. Introduction

2XMM J191043.4+091629.4 is an unclassified X-ray source detected serendipitously by *XMM-Newton* in the vicinity of the Galactic supernova remnant W49B (2XMM; Watson et al. 2009). This X-ray source was discovered with *ASCA*, AX J1910.7+0917, during the survey of the Galactic plane (Sugizaki et al. 2001, who associated it to the *Einstein* source 2E 1908.3+0911). The source was detected by the *INTErnational Gamma-Ray Astrophysics Laboratory* (*INTEGRAL*; Winkler et al. 2003) in the imager *ISGRI* during an observation of the SGR 1900+14 field (Götz et al. 2006, see Fig. 1 in this reference).

INTEGRAL, *ASCA*, *XMM-Newton*, and *Chandra* observations suggested that the source could be a binary transient system associated with the IR counterpart 2MASS J19104360+0916291. The X-ray spectrum seems to be characteristic of a high-mass X-ray binary (HMXB) system with a neutron star as a compact object (although no pulsations have been detected so far; see Pavan et al. 2011). However, neither a classical supergiant wind-fed system nor a Be/X-ray binary fit the observed behaviour well according to Pavan et al. (2011). These authors used the *XMM-Newton* position of the X-ray source to pinpoint the IR counterpart using the 2MASS catalogue and argued that the photometric colours favour a supergiant companion. However, in a deeper search, we found two possible near-IR counterparts in the UKIDSS-GPS DR5 cat-

alogue (United Kingdom Infrared Deep Sky Survey–Galactic Plane Survey: Data Release 5) that were astrometrically coincident with 2.13'' *XMM-Newton* error circle. These two sources appeared unresolved in the 2MASS images that were identified with the 2MASS J19104360+0916291 source (see Fig. 7 in Pavan et al. 2011 and Fig. 1 in Rodes-Roca et al. 2011). This means that the 2MASS photometry is contaminated. We have performed a photometric study of the possible counterparts and have found that the candidate #1 in Fig. 1 is the most likely one. We also obtained reliable photometry.

The source is located in the Galactic plane and has a relatively high absorption in the X-ray domain ($N_H \sim 5 \times 10^{22}$ cm^{-2} , Pavan et al. 2011). The lack of an obvious optical counterpart (Pavan et al. 2011) is also compatible with these characteristics. To advance our current understanding on the nature of AX J1910.7+0917, we used observations in the near-IR range acquired with the *Telescopio Nazionale Galileo* (TNG) 3.5-m telescope. The characterization of the IR counterpart of 2XMM J191043.4+091629.4 is particularly challenging. On one hand the spectral classification of hot stars based on a *K*-band spectrum cannot be completed without ambiguities because of the lack of enough spectral features in that range (Hanson et al. 1996). This problem can be circumvented by combining data for several spectral bands, including the X-rays. On the other hand this system lies in the line of sight of a second (unrelated) star, making it a visual binary with a separation of only 1''. This, together with the strong absorption, requires the use of a 4-m class telescope under very good seeing conditions.

In the framework of an ongoing programme to discover and characterize optical counterparts to HMXBs, we have studied this source. Here, we present observations of the TNG using the Near-Infrared Camera Spectrometer (NICS). According to the near-IR spectral and photometric properties, we propose that the counterpart is most likely an early-type B supergiant star.

2. Observations and data reduction

2.1. The XMM-Newton position and the IR candidate

UKIDSS is a NIR survey covering approximately 7000 deg^2 of the northern hemisphere to a depth of $K = 18 \text{ mag}$, with additional data from two deeper, small-area high-redshift galaxy surveys. Using the Wide Field Camera (WFCAM) on the United Kingdom Infrared Telescope (UKIRT), the survey achieved a pixel resolution of $0.14''$ by use of the micro-stepping technique (see Lawrence et al. 2007, for full details). The data used in this paper were taken from the UKIDSS-GPS, a survey of approximately 2000 deg^2 of the northern Galactic plane in the J , H and K -bands (Lucas et al. 2008). In Figure 1 we show the UKIDSS DR7PLUS Galactic plane survey K -band image of the sky around the position of the X-ray source. As can be seen, the superior spatial resolution of the UKIDSS survey images is able to resolve the 2MASS candidate into two different components, labelled here as #1 and #2. We have also plotted the error circle centred at the best position, namely, $\alpha = 19^{\text{h}} 10^{\text{m}} 43.40^{\text{s}}$ and $\delta = +09^{\circ} 16' 30.0''$, with an error of 2.13 arcsec (Pavan et al. 2011). As can be seen, candidate #2 lies completely outside the error circle and only candidate #1 is compatible with the XMM-Newton position.

2.2. TNG data

Near-IR spectroscopy was obtained from 14-16 July 2012, using the NICS spectrometer at the 3.5-m TNG telescope. The scientific and calibration data were retrieved from the Italian Centre for Astronomical Archive (IA2). Low-dispersion spectroscopy was obtained with the HK grism, which covers the $1.40\text{--}2.50 \mu\text{m}$ spectral region and provides a dispersion of 11.2 \AA/pixel . We note that the component separation is around 1 arcsec, making both spectroscopy and photometry very challenging. For that reason we selected only nights with excellent seeing conditions of $0.75''$ or less. Furthermore, we used a slit of $0.5''$ and oriented it perpendicularly to the line of union of the two stars to acquire only light from the correct candidate, labelled as #1 in Fig 1.

To remove the sky background, the source and the standard stars were observed at several positions along the slit following a dithering ABBA sequence. Consequently, the observation consisted of a series of four images with the source spectrum displaced at different positions along the CCD, using an automatic script available at the telescope. First, cross-talking effects produced by non-saturated images were corrected using the Fortran program available for this purpose. Second, background subtraction was made obtaining our (A–B) and (B–A) image differences. The sequences AB and BA were so close in time that sky background variation between them was negligible. This method, together with the use of the $0.5''$ slit, also minimizes any possible nebular contamination. Third, sky-subtracted images were flat-fielded and the resulting spectra averaged. The wavelength calibration was performed using the Ar lamps available at the telescope. Fitting a third-degree polynomial, the root mean squared error was around 1.7 \AA . Fourth, as telluric calibration source we used A0 V Hip98640 star because this type

of stars is featureless in the K band. Then, we normalized both spectra considering the K band from $2.05 \mu\text{m}$ to $2.2 \mu\text{m}$ and the H band from $1.6 \mu\text{m}$ to $1.75 \mu\text{m}$ by dividing the source spectrum by the standard spectrum to identify the spectral lines of the source. Finally, to minimize the noise, we filtered the high frequencies above the Nyquist frequency $\sigma_N = 1/(2 \cdot \Delta x) = 0.0025 \text{ \AA}^{-1}$ in the Fourier transform of the spectrum, recovering the cleaned spectrum by computing the inverse Fourier transform. The final K-band spectrum is shown in Fig.2.

3. Data analysis

3.1. Near-IR spectrum and classification of the counterpart

The spectral analysis was carried out using the *Starlink*¹ software. To identify the emission/absorption lines and spectral classification, we used the following atlases: Blum et al. (1997), Meyer et al. (1998) and Hanson et al. (1998) for the H band; Hanson et al. (1996) and Hanson et al. (2005) for the K band.

Figure 2 shows the K-band spectrum of the IR counterpart. The presence of He I lines and the absence of He II, which is seen up to O9, points towards a B-type star. The Br γ line is in emission and seems to be blended with the blueward emission of the He I $2.161 \mu\text{m}$ line. We also observe He I $2.058 \mu\text{m}$ in emission as in B supergiants and Be stars. In the atlas of Hanson et al. (2005), no luminosity class III star shows this line in emission. Moreover, we also note the presence of the He I $2.183 \mu\text{m}$ emission line, which becomes apparent in early-B giants, albeit in absorption (see Figs. 5 and 8 to 12 in Hanson et al. 2005).

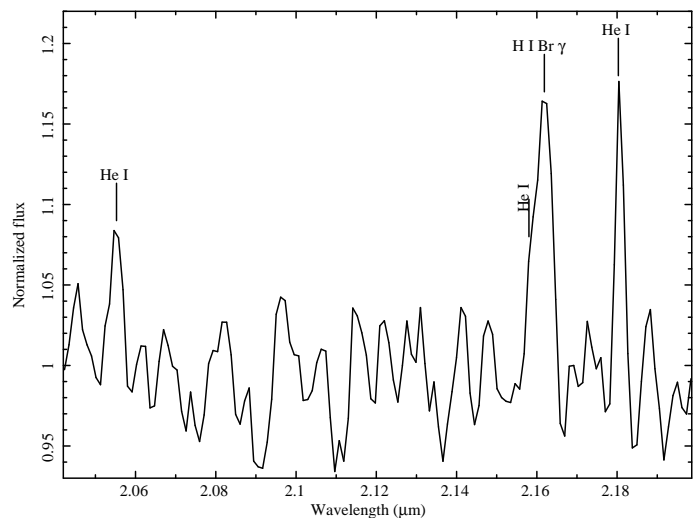


Fig. 2. K-band spectrum of the counterpart to the X-ray binary studied in this work. Note the absence of any feature at the position of the He II $2.1885 \mu\text{m}$ line.

Unfortunately, the low signal-to-noise ratio of the data in the H-band spectrum prevented us from identifying hydrogen lines such as Br10, Br11, or Br12, and/or helium lines like He II $1.6918 \mu\text{m}$ or He I $1.7002 \mu\text{m}$ clearly. Other hydrogen lines are not detected, probably because their intensities would be below the continuum noise level. On the other hand, cool supergiant stars show CO-band absorption lines between 2.29 and $2.35 \mu\text{m}$ that are not present in our spectrum. We therefore rule out a late-type companion for 2XMM J191043.4+091629.4.

¹ <http://starlink.jach.hawaii.edu/starlink>

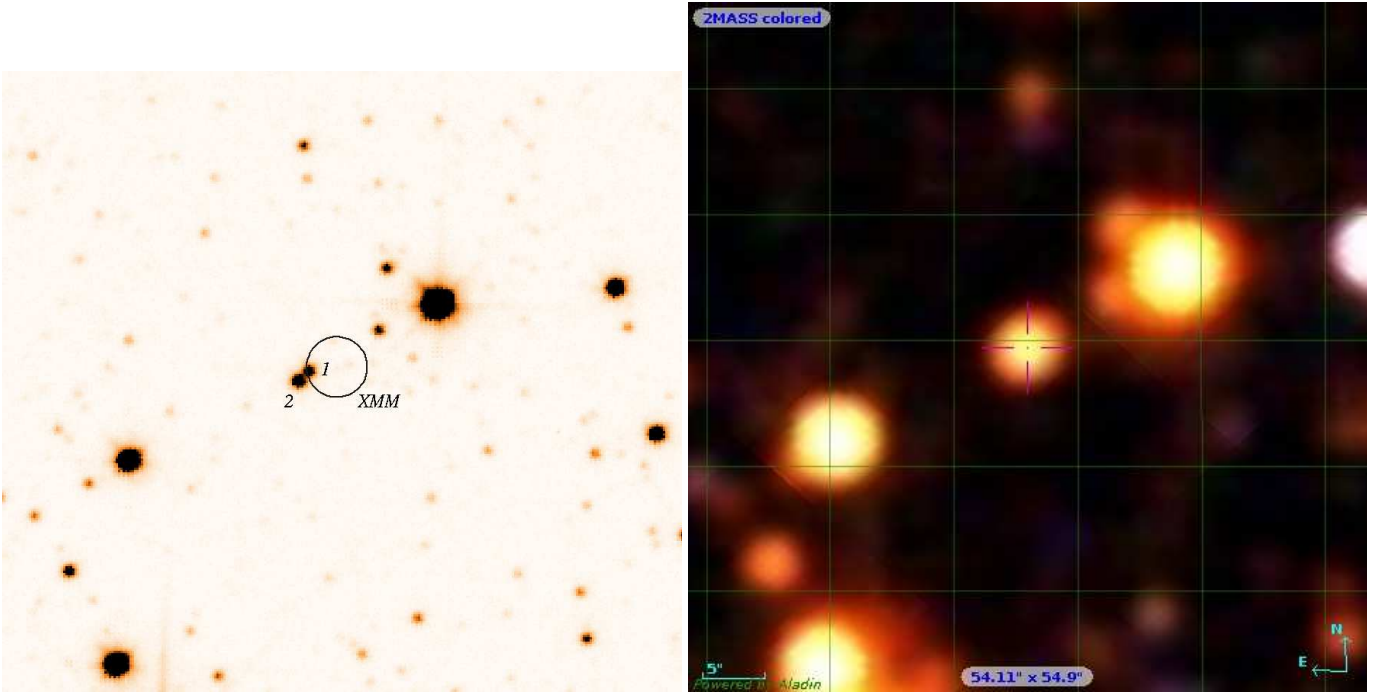


Fig. 1. *Left panel:* $15'' \times 15''$ K finding chart for 2XMM J191043.47+091629.4. The black circle is centred on the *XMM-Newton* position of 2XMM J191043.47+091629.4, with the radius indicating the 2.13'' positional error. *Right panel:* $3.6' \times 2.6'$ 2MASS coloured map. The images are displayed with north up and east to the left. We note that the two NIR UKIDSS sources appear unresolved in the 2MASS image.

In conclusion, the spectral type corresponds to an early-B star while the luminosity class can not be constrained from the near-IR spectrum and is consistent with either class I (supergiant) or class V (Be star). In the following, however, we argue that the X-ray characteristics of the source are more compatible with a supergiant X-ray binary system.

3.2. IR photometry

To carry out the photometric analysis of the images we used the *Starlink* software, in particular the Graphical Astronomy and Image Analysis Tool (*GAIA*) package. As shown in previous sections, the 2MASS candidate is actually an unresolved pair. Therefore the 2MASS photometry for this candidate is contaminated and cannot be used to compute the distance to the source. We used the UKIDSS images instead (see Fig. 3). In the UKIDSS database only the K magnitude for candidate #1 is available ($K = 13.135 \pm 0.003$), because the counterpart is very weak and the automatic extraction only gives a poor solution. However, the counterpart is clearly visible also in H - and J images, although barely in this last band. To perform the photometry, we extracted the fluxes of candidate #1 as well as those of several dozens of other stars seen in the image using synthetic aperture photometry. Background fluxes were also extracted from source-free regions in the same image, close to the different stars. The instrumental magnitudes were then correlated with the corresponding magnitudes available at the UKIDSS database. Finally, the calibration equations were applied to the fluxes of candidate #1 to obtain the photometry given in Table 1.

As a consistency check, the K magnitude obtained from the direct application of the previous calibrated equations to source #1 was identical, within the errors, to that quoted in the UKIDSS database. Therefore, the magnitudes and errors given in Table 1

J	H	K
≥ 17.1	14.43 ± 0.05	13.135 ± 0.003

Table 1. Photometry of candidate #1 in the UKIDSS system.

are reliable. No error is given for the J magnitude because source #1 is already very weak in this band and only an upper limit can be obtained. Clearly, the source is strongly reddened.

Assuming a B0I type, the intrinsic colour would be $(H - K)_0 = -0.08$ (Ducati et al. 2001). Now using the photometry in Table 1, we can estimate an infrared excess of $E(H - K) = 1.30$. This corresponds to an $E(B - V) = E(H - K)/0.17 = 7.6 \pm 0.3$ (Fitzpatrick 1999). This high value agrees with the column density deduced from the X-ray analysis ($N_H = 6 \times 10^{22} \text{ cm}^{-2}$; Pavan et al. 2011), which would correspond to an $E(B - V) = 8.8$ (Ryter 1996). This last value is obtained assuming that the entire column is interstellar but, in fact, part of it will be local if the compact object is embedded in the companion's wind. Note that a later spectral type would reduce the value of the total reddening $E(H - K)$ still more, and owing to the spectral analysis of the previous section, we can rule out a late-type companion. The available data then are more consistent with an early-type companion. The total-to-selective absorption will be $A_K = 0.36 E(B - V) = 2.74$. Now, assuming an absolute magnitude $M_K = -5.6$ for a B0I star, this would translate into a distance to the source of $d = 16.0 \pm 0.5$ kpc.

On the other hand, Bry is the most prominent feature in Be stars in the K band, while He I $2.058 \mu\text{m}$ is found in early-type Be stars, up to B2.5 (Clark and Steele 2000). Therefore, assuming a B0V star, the intrinsic colour would be $(H - K)_0 = -0.05$ (Ducati et al. 2001) and $E(H - K) = 1.27$, also compatible with the X-ray column density. The $M_K = -3.17$ and the corresponding distance $d = 5.3$ kpc. From the analysis of X-ray data

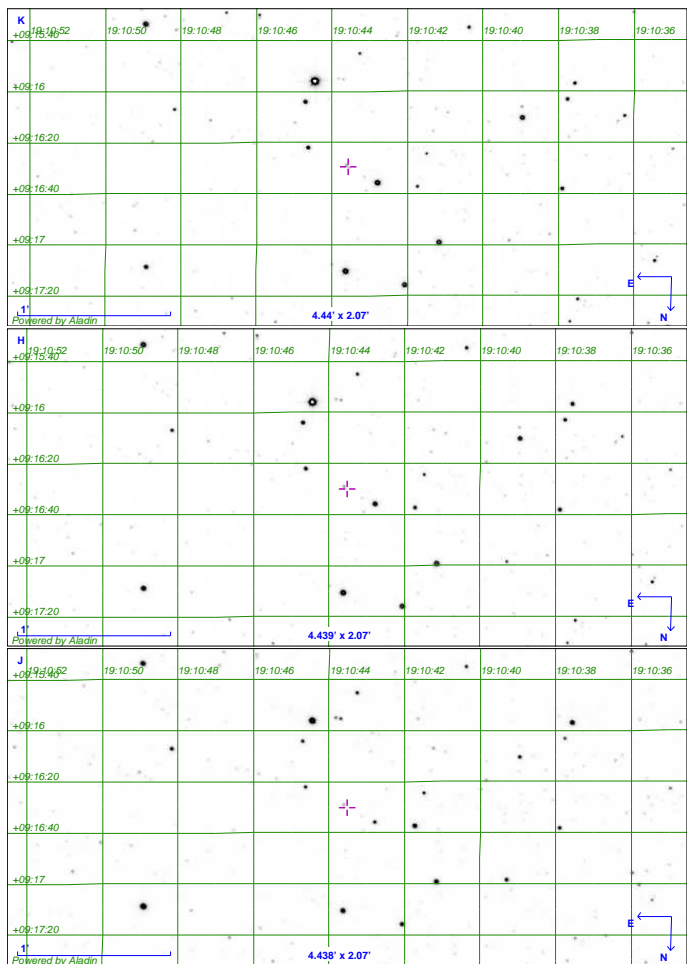


Fig. 3. $4.4' \times 2.1'$ *K* (top), *H* (middle), and *J* (bottom) finding chart for 2XMM J191043.47+091629.4. The cross is centred on the *XMM-Newton* position of 2XMM J191043.47+091629.4. The UKIDSS image is displayed with north down and east to the left.

(Pavan et al. 2011), the average unabsorbed flux is of the order of $2 \times 10^{-11} \text{ erg s}^{-1} \text{ cm}^{-2}$. At a distance of 5.3 kpc this would translate into an X-ray luminosity of $L_X = 6.7 \times 10^{34} \text{ erg s}^{-1}$. This is two to three orders of magnitude lower than the typical luminosities for type I outbursts in transient BeX-ray binaries (BeXBs). On the other hand, there is a growing class of systems called persistent BeXBs that are characterized by low X-ray luminosities, $L_{(2-20) \text{ keV}} \sim 10^{34-35} \text{ erg s}^{-1}$ (Reig 2011). These systems are relatively quiet, showing flat light curves with sporadic and unpredictable increases in intensity by less than one order of magnitude, and very weak, if any, iron fluorescence line at $\sim 6.4 \text{ keV}$. The upper limit on the X-ray flux in quiescence of the source AX J1910.7+0917 (1–10 keV energy band) is $5.4 \times 10^{-11} \text{ erg s}^{-1} \text{ cm}^{-2}$ (Pavan et al. 2011 from a *Chandra* observation), implying an X-ray luminosity during quiescence of $L_{(1-10) \text{ keV}} \lesssim 1.8 \times 10^{33} \text{ erg s}^{-1}$, which is below the limit displayed by the persistent BeXBs discovered so far. Therefore, the X-ray observations are inconsistent with a classical transient BeXB, but could be compatible with a low-luminosity persistent BeXB.

Finally, the *K*-band spectrum, which shows narrow emission lines due to He I and Bry (Howell et al. 2010), would be compatible with those displayed by CVs. But, again, this possibil-

ity is ruled out by the X-ray emission characteristics from AX J1910.7+0917 as discussed in Pavan et al. (2011).

We also searched for a possible $H\alpha$ emission from the system using Isaac Newton Telescope Photometric $H\alpha$ Survey (IPHAS, Drew et al. 2005). We followed the Euro-Virtual Observatory (VO) scientific case developed by Zolotukhin & Chilingarian (2011). We were able to select 23 IPHAS sources inside a 1.3 arcmin circular field around the *XMM-Newton* best position. Using VO tools, namely CDS ALADIN (Bonnarel et al. 2000) and TOPCAT (Taylor 2005), we explored the colour-colour diagram of the IPHAS sources (see Fig. 4).

The straight line in Fig. 4 roughly corresponds to main-sequence stars, which do not exhibit $H\alpha$ emission, while outlier points correspond to $H\alpha$ emitters. We found a single detectable prominent $H\alpha$ emitter whose coordinates $\alpha = 19^h 10^m 42.94^s$ and $\delta = +09^\circ 16' 01.6''$ are outside the $2.13''$ *XMM-Newton* error circle, however (the difference between the coordinates is $\Delta\alpha = 10.4''$ and $\Delta\delta = 28.4''$, implying an angular separation from the *XMM* source position of $30.2''$). The non-detection of $H\alpha$ emission from the system is not strange, though. In the previous section, we derived a reddening value of $E(B - V) = 7.6$, implying an extremely high extinction in *R* ($A_R \sim 16 \text{ mag}$) and *I* ($A_I \sim 12 - 13 \text{ mag}$). It is therefore expected that IPHAS has no detections inside the *XMM-Newton* error circle since the object is already very faint in *J*.

In conclusion, the most likely counterpart to 2XMM J191043.4+091629.4 is an early-type B I star located at a distance² of $d = 16.0 \pm 0.5 \text{ kpc}$, placing this source in the Outer Arm.

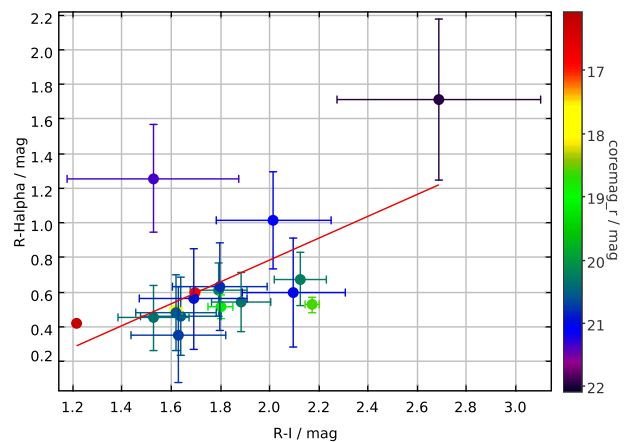


Fig. 4. Colour-colour diagram of the IPHAS detections (not sources) in the 1.3 arcmin field around *XMM-Newton* coordinates. Objects with $H\alpha$ excess are located towards the top of the diagram. The *r* magnitude is colour-coded.

4. Summary and discussion

According to the previous analysis, we have identified the counterpart to 2XMM J191043.4+091629.4 as being a B supergiant star. This implies that 2XMM J191043.4+091629.4 belongs to

² The error would be $\pm 0.3 \text{ kpc}$ if we assumed a 0.5 magnitude error in the absolute magnitude calibration for early-type supergiants

the class of obscured HMXBs that has been unveiled in the past decade by satellites such as *INTEGRAL*. A large fraction show intrinsically high absorption along the line of sight ($N_H \gtrsim 10^{23} \text{ cm}^{-2}$ Kuulkers 2005). These IGR sources share similar X-ray properties typical for accreting X-ray pulsars in HMXBs. The unabsorbed X-ray luminosity in the energy range 2–100 keV in of the order 10^{35} – $5 \times 10^{36} \text{ erg s}^{-1}$ is also typical for HMXBs. In addition, the vast majority of these newly discovered sources had supergiant donors.

Assuming a distance to the source 2XMM J191043.4+091629.4 of 16.0 kpc (see Sect. 3.2) and isotropic emission, the estimated X-ray luminosity is $(0.9\text{--}1.3) \times 10^{36} \text{ erg s}^{-1}$ in the 0.3–10.0 keV range. Moreover, the photon index $\Gamma \sim 1.2$, and the $N_H \sim 0.5 \times 10^{23} \text{ cm}^{-2}$ are also consistent with the characteristics of the new population of highly absorbed supergiant HMXBs. This is compatible also with the lower band of the typical X-ray luminosity of *classical* supergiant X-ray binaries (SGXBs) such as Vela X-1 or 4U 1538–52, which is of the order of $L_X \approx 10^{36} \text{ erg s}^{-1}$.

Moreover, the source is heavily obscured, with an $E(B-V) = 7.6$ implying extinctions of about $A_V \sim 23.6$ mag in the visual band. At an estimated distance of 16.0 kpc, the source would be located in the Outer Arm. The line of sight, then, crosses the heavily populated Perseus arm and, perhaps, the Sagittarius arm tangent, which explains the high extinction displayed by the system. On the other hand, with the data at hand we cannot discard completely a persistent BeXB which, located at $d = 5.3$ kpc, would be the faintest ($L_X \approx 10^{33} \text{ erg s}^{-1}$) found so far, however.

Until *INTEGRAL* discovered supergiant fast X-ray transients (SFXTs) and highly absorbed supergiant X-ray binaries (SGXBs), the population of these systems was relatively small, in agreement with evolutionary scenarios. Most of them were known because they were persistent, moderately bright X-ray sources. These class of systems are growing and, currently, *INTEGRAL* has discovered more SGXBs than were previously known (Walter et al. 2006). This discovery means a substantial challenge to binary star population synthesis models, which try to reproduce the observed abundances of different types of binaries. This source will add to the growing population of heavily obscured sources. In addition, this system contributes to tracing the structure of the scarcely explored Outer Arm of our Galaxy.

Acknowledgements. We would like to thank the anonymous referee for the valuable suggestions that improved the quality of the paper. This work was supported by the Spanish Ministry of Education and Science project number AYA2010-15431, *De INTEGRAL a IXO: binarias de rayos X y estrellas activas*. Based on observations made with the Italian Telescopio Nazionale Galileo (TNG) operated on the island of La Palma by the Fundación Galileo Galilei of the INAF (Istituto Nazionale di Astrofisica) at the Spanish Observatorio del Roque de los Muchachos of the Instituto de Astrofísica de Canarias in Director Discretionary Time. JJRR acknowledges the support by the Spanish Ministerio de Educación y Ciencia under grant PR2009-0455.

References

- Blum, R. D., Raymond, T. M., Conti, P. S. et al. 1997, *AJ*, 113, 1855
 Bonnarel, F., Fernique, P., Bienaymé, O. et al. 2000, *A&AS*, 143, 33
 Clark, J. S. & Steele, I. A. 2000, *A&ASS*, 141, 65
 Drew, J. E., Greimel, R., Irwin, M. J. et al. 2005, *MNRAS*, 362, 753
 Ducati, J. R., Bevilacqua, M. C., Rembold, S. B. et al. 2001, *ApJ*, 558, 309
 Fitzpatrick, E. L. 1999, *PASP*, 111, 63
 Götz, D., Mereghetti, S., Tiengo, A. et al. 2006, *A&A*, 449, L31
 Hanson, M. M., Conti, P. S. & Rieke, G. H. 1996, *ApJS*, 107, 281
 Hanson, M. M., Rieke, G. H. & Luhman, K. L. 1998, *AJ*, 116, 191
 Hanson, M. M., Kudritzki, R. P., Kenworthy, M. A. et al. 2005, *ApJS*, 161, 154
 Howell, B. S., Harrison, T. E., Szkody, P. et al. 2010, *ApJ*, 139, 1771
 Kuulkers, E. 2005, in "Interacting binaries: Accretion, evolution and outcomes", *AIP Conf. Proc.*, 797, 402

- Lawrence, A., Warren, S. J., Almaini, O. et al. 2007, *MNRAS*, 379, 1599
 Lucas, P. W., Hoare, M. G., Longmore, A. et al. 2008, *MNRAS*, 391, 136
 Meyer, M. R., Edwards, S., Hinkle, K. H. et al. 1998, *ApJ*, 508, 397
 Pavan, L., Bozzo, E., Ferrigno, C. et al. 2011, *A&A*, 526, A122
 Reig, P. 2011, *Ap&SS*, 332, 1
 Rodes-Roca, J. J., Torrejón, J. M., Farrell, S. et al. 2011, in Proceedings of the 33rd Reunión Bienal de la Real Sociedad Española de Física, Volum IV, 38
 Ryter, Ch. E. 1996, *Ap&SS*, 236, 285
 Sugizaki, M., Mitsuda, K., Kaneda, H., et al. 2001, *ApJS*, 134, 77
 Taylor, M. B. 2005, in *Astronomical Data Analysis Software and Systems XIV*, ed. P. Shopbell, M. Britton & R. Ebert, *ASP Conf. Ser.*, 347, 29
 Walter, R., Zurita Heras, J., Bassani, L. et al. 2006, *A&A*, 453, 133
 Watson, M. G., Schröder, A. C., Fyfe, D. et al. 2009, *A&A*, 493, 339
 Winkler, C., Courvoisier, T. J.-L., Di Cocco, G., et al. 2003, *A&A*, 411, L1
 Zolotukhin, I. Y. & Chilingarian 2011, *A&A*, 526, A84